



Journal of Applied Sciences

ISSN 1812-5654

science
alert

ANSI*net*
an open access publisher
<http://ansinet.com>

Internal Model Controller of an ANN Speed Sensorless Controlled Induction Motor Drives

Ben Hamed Mouna and Sbita Lassaâd
Research Unity of Modeling, Analyze and Control Systems,
National Engineering School of Gabés (Enig), Tunisia

Abstract: This study deals with the performance analysis and implementation of a robust sensorless speed controller. The robustness is guaranteed by the use of the Internal Model Controller (IMC). An intelligent algorithm is evolved to eliminate the mechanical speed. It is based on the Artificial Neural Network (ANN) principle. Verification of the proposed robust sensorless controller is provided by experimental realistic tests on a scalar controlled induction motor drive. Sensorless robust speed control at low speeds and in field weakening region (high speeds) is studied in order to show the robustness of the speed controller under a wide range of load.

Key words: Robust speed control, induction motor, scalar control, sensorless operation, artificial neural network, IMC

INTRODUCTION

Induction motors are relatively inexpensive and rugged machines. Consequently much attention has been given to induction motor control for starting, standstill, speed reversal, position control... etc.

The induction motor torque is dependent both on the flux and the speed. But neither relationship is linear. A fact that complicates the design of the control system for induction machines. Thanks to scalar and field orientation controls, induction machines are used in a various industrial applications (Metwally *et al.*, 2002).

Not only the coupling behavior of the induction motor represents a great problem but also the variation of its parameters mainly with the temperature (Constantine *et al.*, 2006). Researchers have used various types of closed loop controllers for the rotor speed of the induction motor. Among these controllers, the proportional integral derivative controllers are widely used in the outer speed loop. However, the use of this type of controllers is more sensitive to parameter variation. To overcome this problem, adaptative and robust controls were used. The adaptative control requires a great deal of computation while H_{∞} robust control requires the knowledge of the limit of the disturbance (Duc and Font, 1999; Oustaloup, 1994; Ben Salem and Sbita, 2006a, b). The sliding mode control is also used in the speed loop but the biggest drawback of this type of controller is the high switching frequency (Lai and Shyu, 2005). Recently, speed controllers based on artificial intelligence techniques such as fuzzy logic

and neural network based controllers have been proposed (Sbita and Ben Hamed, 2007; Fonseca *et al.*, 1999; Denai and Attia, 2002). Since these approaches do not require the knowledge of a mathematical machine model, the algorithm would remain robust despite parameter deviations and noise measurements. However, the computational expenses and the need for expert knowledge of the system setup have seriously restricted their applications in practice.

All high performance scalar controlled induction motor drives require accurate rotational speed information for feedback control. This information is mainly provided by incremental encoder. The use of this sensor implies more electronics, high cost and increase in electrical susceptibility. To overcome these problems, a speed observer has to be included in the control loop.

In this study, an internal model controller is developed for the feedback of the scalar controlled induction motor. This IMC controller has the advantage of robustness, ease of design and good speed responses. To cope with the sensor's problem, an alternative algorithm that realizes a quick and accurate speed sensing of the induction motor speed control is carried out. ANN with three layers is used with offline training. The data used for training are obtained when the motor is working in closed loop at various values of speed and loads.

Performances of the developed sensorless speed controller and its accuracy are verified through series of experiments. These consist of step, acceleration and deceleration at low speeds and in a field weakening region, under both unload and loaded conditions.

Proposed scheme of the drive system: The block diagram of the proposed induction motor drive system is shown in Fig. 1. The closed loop control scheme of the induction motor is based on the internal model controller for the rotor speed. The strategy to assume the decoupling of the induction motor is scalar control using voltage source inverter.

Neural network speed observer: The artificial neural network technique is based on a learning process (Heredia *et al.*, 2001; Dreyfus *et al.*, 2002). Neural networks have the advantages of extremely fast parallel computation and fault tolerance characteristics due to disturbance of network intelligence (Hwan *et al.*, 2001). Many neurons or processing elements are interconnected to form a parallel network. Each element or neuron is a very simple processor that carries out the pondered sum of its inputs and applies them to a function (linear, sigmoid) to generate an output that is sent to another neuron.

Generally, the back propagation method is used for adjusting the neural network weights during the training. This process requires a high consumption of time since the algorithm is highly time consuming to converge to the desired error. This phase is usually made off line.

Using an artificial neural network, it is possible not to depend on approximate models since the net learns from a complete and real model. The use of a neural network to observe the speed consists of an association of some inputs with some outputs. In this case, for each set of inputs, there is a set of outputs. To accomplish this operation, the net will have to be trained in a first phase. It is not necessary to carry out this phase in real time and give the net all possible inputs-outputs combinations since it has the capacity to generalize results starting from

a limited set of inputs outputs. Once the phase of training has been accomplished, the net is prepared to observe the speed for any set of inputs.

During the training process, we have experimented with different architectures and learning methods. The objective is to find a compromise between the convergence speed and the target error. The most significant points to keep in mind when defining the structure and operation of a neural nets is mainly the choice of the inputs and outputs. Some inputs should be chosen that determine completely the rotor speed of the induction motor. The inputs in the motor must be easily measured so that the used hardware for induction motor control will be simplified.

It is known with the help of many experiments that for each value of the control voltage (the output of the internal model controller, u) and phase stator current corresponds one value of the rotor speed. Therefore, the appropriate parameters that can be used to detect thoroughly the rotor speed are the control voltage (u) and stator phase current (I_s). Compared with other studies (Jamie *et al.*, 1994; Ben Hamed and Sbita, 2006; Kubota, 1993), this method reduces the number of sensors used to achieve this aim to single one (current sensor). It is better to obtain a neural network speeds observer which observes the whole range of speeds (from negative to positive values). By looking at extent training data, we find them very huge and the neural network observer finds many training problems because of amount of informations to be learnt by the neural network. Many solutions are proposed (Heredia *et al.*, 2001; Hwan *et al.*, 2001). For example, we can increase the number of layers and neurons. However, this creates a problem of computation time and memory capacity. A simple and easy solution is to learn only the range of the

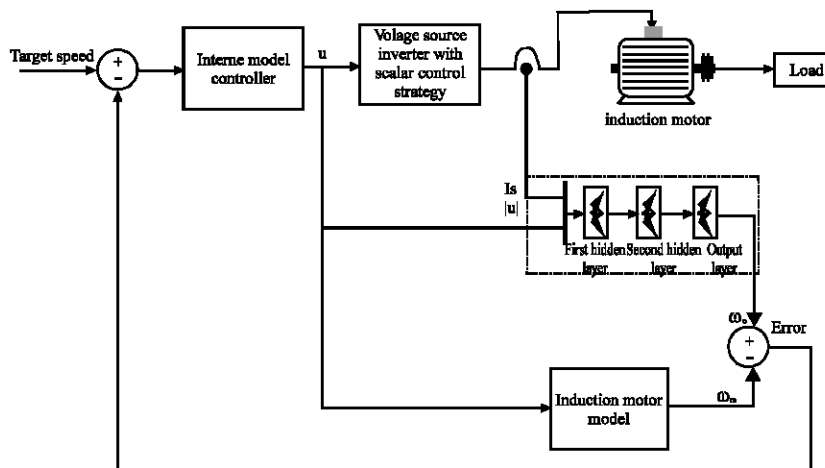


Fig. 1: Block diagram of sensorless induction motor drive

positive speed. It is known that the relation between positive and negative speeds is a minus mark in the command issue. How to detect the negative speeds? If the reference speed becomes negative, the speed becomes also negative and vis versa. To make the neural network available in negative speeds, an absolute value is added to the control voltage and a sign function is implemented. Using this technique, we save time, memory capacity and we observe the speed in the whole range (from positive to negative).

The final structure of the neural network used is a multilayer net with the three layers. The sigmoid function has an output signal varying between 0 and 1. Therefore, we adopt the signals by dividing the output by its nominal value. The way of training the neural network consists of taking the training data corresponding to the positive speed and presenting these pieces of information to the back propagation algorithm.

The training algorithm of the neural network speed observer is as follows:

- 1st step: Initially randomize the weights from -0.5 to 0.5,
- 2nd step: Obtain the control voltage from the internal model controller and the stator current from the sensor (vector data is saved in a closed loop),
- 3rd step: Calculate the error between real and observed speed,
- 4th step: Adjust the weights of the neural network,
- 5th step: Calculate the output of the neural network,
- 6th step: Repeat 2nd step until the stipulated error is reached.

The internal structure of the neural network observer is shown in Fig. 2.

Scalar control induction motor: Scalar control strategy is determined under steady state condition. Relying on the

mathematical equations governing the electrical dynamics of an induction motor in a synchronous rotating frame in steady state (Zidani *et al.*, 2002), we obtain:

$$\vec{v}_s = r_s \vec{i}_s + j\omega_s \vec{\Phi}_s \tag{1}$$

$$\vec{v}_r = r_r \vec{i}_r + j(\omega_s - \omega) \vec{\Phi}_r \tag{2}$$

In the following section, we use the well known equivalent monophasic model transformed to the stator where we consider that the magnetic leakages are totalized and grouped in the rotor and designed by $N_e \omega_s$. Figure 3 shows this model (Grellet and Clerc, 1996).

In this figure, R'_r and N_e represent the rotor resistance and total leakage inductance located in the rotor, respectively.

The evolution of the stator synchronous field around the rotor produces an electromagnetic power which will be transmitted to the rotor at synchronous speed. The electromagnetic power is defined as:

$$P_{em} = T_{em} \Omega_s = 3 \frac{R'_r}{g} \frac{V_s^2}{\left(\frac{R'_r}{g}\right)^2 + (N_e \omega_s)^2} \tag{3}$$

Assuming that the stator resistance is negligible, we obtain:

$$T_{em} = 6\pi \Phi_s^2 \frac{\frac{R'_r}{f_r}}{\left(\frac{R'_r}{f_r}\right)^2 + (N_e 2\pi)^2} \tag{4}$$

Where f_r is the slip frequency.

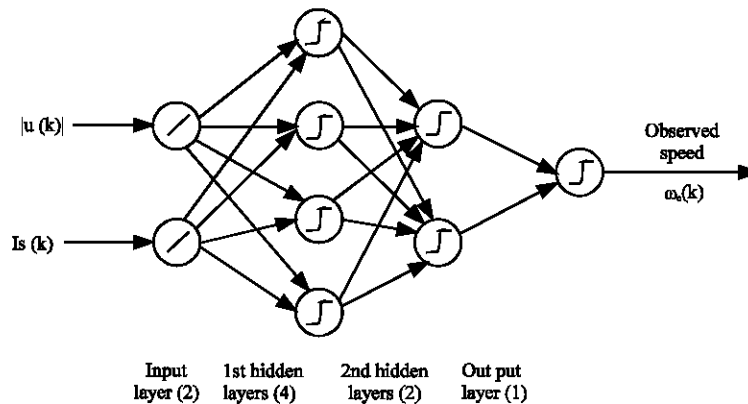


Fig. 2: The internal structure of the neural network observer

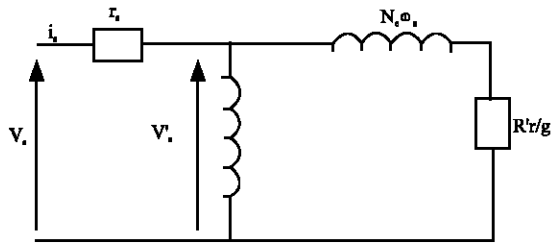


Fig. 3: Block diagram of the equivalent monophasic induction motor model

The mechanical dynamic of the induction motor is expressed as:

$$J \frac{d\omega}{dt} = p(T_{em} - T_L) \tag{5}$$

If the load torque (T_L) is set equal to zero, the transfer function which defines the relation between the rotor speed ω and ω_s will be given as:

$$\frac{\omega}{\omega_s} = \frac{3p^2\Phi_s^2}{R_r' J s + (R_r' f + 3p^2\Phi_s^2)} = \frac{k}{1 + \tau s} \tag{6}$$

Here p is the number of pole pairs, f the viscous coefficient, τ the time constant and k the static gain of the system.

Hence, the scalar induction motor model is represented by a first order system. To identify the characteristics of this system model, a standard recursive least square method is used.

Identification with recursive least square algorithm: The recursive least square identification algorithm is described by the following steps (Koubaa, 2004):

- Initial conditions: the initial value of the estimated parameter vector $\hat{\theta}$ is set equal to zero. The initial covariance matrix is assumed to be diagonal with large positive numbers.
- Compute estimate $\hat{y}(k)$

$$\hat{y}(k) = \hat{\theta}^T(k-1)x(k) \tag{7}$$

- Compute the estimation error of $y(k)$

$$\varepsilon(k) = y(k) - \hat{\theta}^T(k-1)x(k) \tag{8}$$

- Compute the estimation covariance matrix at instant k

$$P(k) = P(k-1) - \frac{P(k)x(k)x^T(k)P(k-1)}{1+x^T(k)P(k-1)x(k)} \tag{9}$$

- Compute the estimation vector at instant k

$$\hat{\theta}(k) = \hat{\theta}(k-1) + P(k)x(k)\varepsilon(k) \tag{10}$$

- Repeat steps 2-5 until the iteration number (measurement number) or error value is reached.

Identification of steady state induction motor model with recursive least square algorithm: The discrete induction motor model is defined as:

$$G(z) = \frac{\hat{b}z^{-1}}{1 + \hat{a}z^{-1}} = \frac{\hat{y}(k)}{u(k)} \tag{11}$$

Based on (28), the recurrent equation is given by:

$$\hat{y}(k) = \hat{b}u(k-1) - \hat{a}y(k-1) \tag{12}$$

This can be written as:

$$y(k) = \hat{\theta}^T(k)x(k) \tag{13}$$

$\hat{\theta}$ is the vector of estimated parameters and the regression vector containing the old inputs and outputs of the system that need to be identified.

Here $\hat{\theta}$ and x are defined as:

$$\hat{\theta}(k) = [\hat{b} \quad \hat{a}]^T \tag{14}$$

$$x = [u(k-1) \quad -y(k-1)] \tag{15}$$

To identify the estimated parameters, an experimental test was carried out on a 1kw induction motor scalar drive system. It is excited with a Pseudo Random Binary Sequency (PRBS) in order to obtain a data file input output measurement and an off line identification based on the standard recursive least square is done. The evolution of the output and input measurements is shown in Fig. 4. while Fig. 5 presents the identification results.

Based on these results, the final discrete function can be written as:

$$G_m(z) = \frac{bz^{-1}}{1 + az^{-1}} = \frac{\omega(k)}{\omega_s(k)} \tag{16}$$

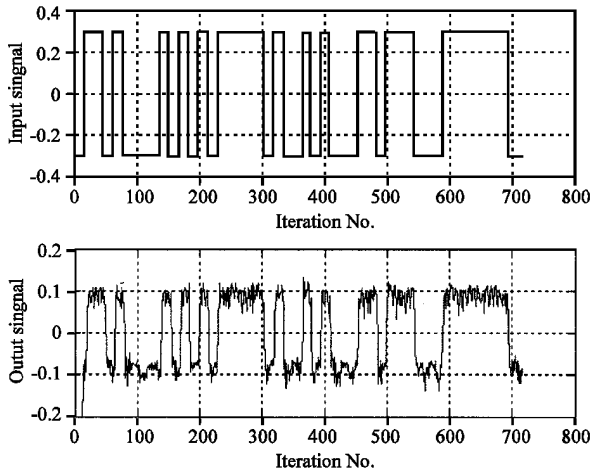


Fig. 4: Evolution of the input and the output signals

With $b = 0.0611$ and $a = -0.8254$.

Validity of the established discrete induction motor model: The principle of this test is illustrated by the following steps:

- Compute the quantity defined as:

$$RN(i) = \frac{\sum_{k=1}^N \varepsilon(k)\varepsilon(k-i)}{\sum_{k=1}^N \varepsilon^2(k)}, \text{ if } i > 1. \quad (17)$$

$I = \sup (n_a, n_b + d)$ with n_a the order of the denominator and n_b is the order of the numerator.

- Verify the condition validity given as:

$$|RN(i)| \leq \frac{2.17}{\sqrt{N}} \quad (18)$$

In our application, $N = 716$. Then, we get $|RN(I)| \leq 0.0811$.

The theoretical computation leads to:

$$\begin{aligned} RN(0) &= 1, \\ RN(1) &= -0.0733, \\ RN(2) &= -0.0544, \\ RN(3) &= -0.0466, \end{aligned} \quad (19)$$

As shown by these results, the condition (35) is already verified. Therefore, we conclude that the established induction motor model is valid.

Internal model controller: The speed controller is based on the principle of internal model control which makes it robust and immune to disturbances (parameter variations and external load torque disturbance) (Shao *et al.*, 2005). The internal model controller consists mainly of the controller and system model (16). The block diagram of the internal model controller structure is given by Fig. 6 (Borne *et al.*, 1998; Abdunnaser and Ali Milad, 2005).

When the process is linear and so as, it can be described by a transfer function $G(z)$, based on the bloc diagram of the internal model controller (Fig. 6). Therefore, we establish the following:

$$y(z) = G(z)u(z) + D(z) \quad (20)$$

$$ym(z) = Gm(z)u(z) \quad (21)$$

The command $u(z)$ is expressed as:

$$u(z) = Q(z) \left[[yc(z) - (G(z) - Gm(z))u(z)] - D(z) \right] \quad (22)$$

It can be simplified as:

$$u(z) = [1 + Q(z)(G(z) - Gm(z))]^{-1} Q(z) [yc(z) - D(z)] \quad (23)$$

Where $yc(z)$ denotes the target value of the output value $y(z)$.

Replacing $u(z)$ with its value in (36) yields

$$y(z) = G(z) [1 + Q(z)(G(z) - Gm(z))]^{-1} Q(z) [yc(z) - D(z)] + D(z) \quad (24)$$

Here, we distinguish two circumstances depending on whether the modeling system is perfect or not. If it is perfect, then $G(z) = Gm(z)$. Using this condition, we obtain:

$$y(z) = G(z)Q(z)[yc(z) - D(z)] + D(z) \quad (25)$$

The aim is to assume that $y(z) = yc(z)$ in steady state both for tracking and regulation. It is clear that if we choose $Q(1) = 1/G(1)$, then $y(\infty) = yc(\infty)$ when k goes to infinity. Writing $Q(1) = 1/G(1)$ is valid only if the process is stable.

If the modeling system is not perfect, a low pass filter $F(z)$ should be added in order to eliminate the effect of the modeling error. In this case:

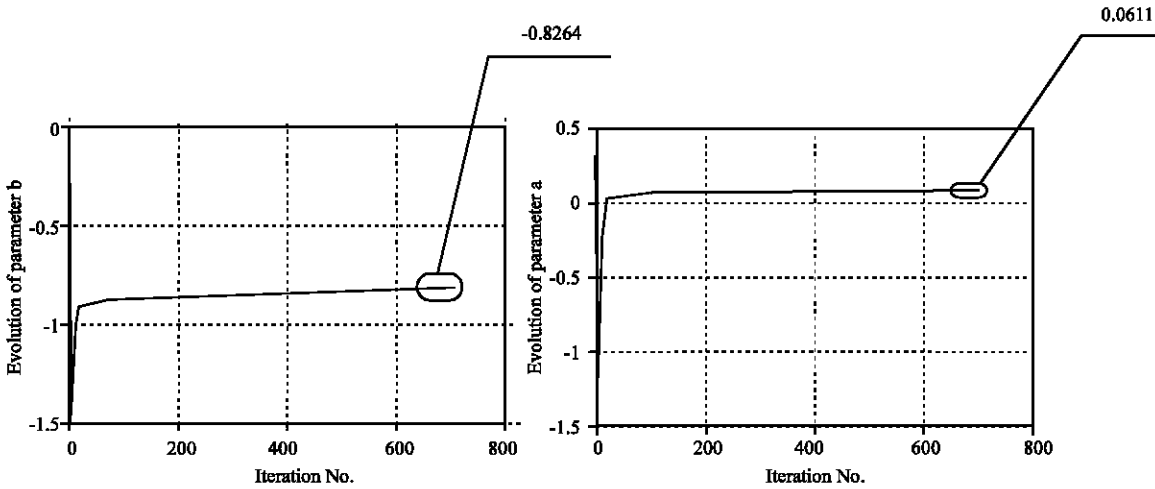


Fig. 5: Evolution of the identification parameters

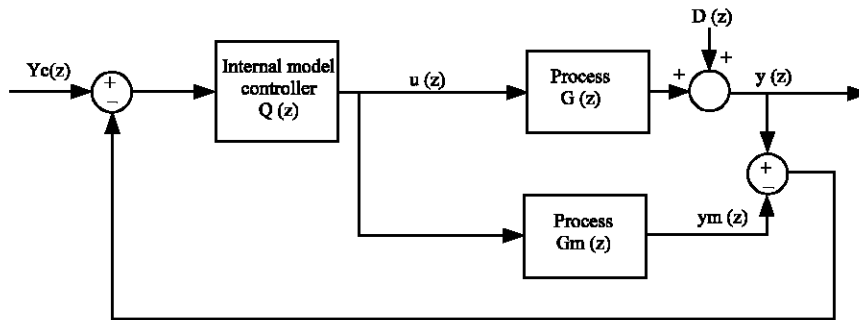


Fig. 6: Block diagram of internal model control

$$y(z) = G(z) [1 + Q(z)F(z)(G(z) - G_m(z))]^{-1} Q(z)[y_c(z) - F(z)D(z)] + D(z) \quad (26)$$

From this equation, it is clear that to eliminate the disturbance and assume $y(\infty) = y_c(\infty)$ when k goes to ∞ , we must choose The easy way is to choose a low pass filter with a unit static gain.

In reality, the low pass filter is used not only to eliminate the modeling error but also to make the controller physically realizable. It has an adjustable parameter that can be adjusted on line and off line in order to make the internal model controller more robust when it comes modeling errors. Hence, the final form of the internal model controller is given as:

$$Q(z) = Q_0(z)F(z) \quad (27)$$

The model internal controller is applied only for stable systems. In order to obtain the final form of the internal model controller, five steps are to be followed:

Step 1: The zeros of $Q_0(z)$ are the poles of the model system.

Step 2: The poles of $Q_0(z)$ are chosen as

- The stable zeros of the model system,
- The reverse of the instable zeros of the model system,
- A zero pole is added at each zero with a negative real part,

Step 3: Zero pole is added to $Q_0(z)$,

Step 4: To obtain a zero error in the steady state, the controller gain is chosen so that equals one,

Step 5: A low pass filter is added in order to overcome the problems caused by the modeling error. In general (Flaus, 2000):

$$F(z) = \frac{(1-\alpha)z}{z-\alpha} \quad (28)$$

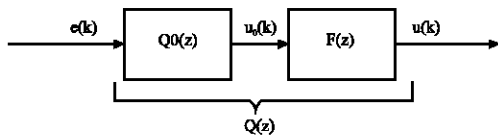
Where $0 < \alpha < 1$.

The robustness of this controller is achieved by choosing to right α value

The final form of the IMC controller can be written as:

$$Q(z) = Q_0(z)F(z) \quad (29)$$

Which can be represented as:



Now, in order to determine $u(k)$, we calculate the product of $F(z)$ and $u_0(k)$. Therefore, we obtain:

$$u(k) = F(z)u_0(k) \quad (30)$$

Replacing $F(z)$ with its value, Eq. 46 yields:

$$u(k) = \alpha u(k-1) + (1-\alpha)u_0(k) \quad (31)$$

If α is close to 1 (1-converges to zero), then, $u(k)$ remains close to $u(k-1)$ although the difference process model occurs which proves the robustness of this controller. Hence the process dynamic in closed loop is fixed by this filter parameter. Several experimental tests were carried out to tune the filter parameter while trying to make a compromise between the rapidity and stability for the overall system. The final value used is, then, fixed to 0.9.

The condition of the internal model control is justified by the nyquist locality shown in Fig. 7. Based on the Nyquist criterion which announces that a necessary and sufficient stability condition is that the round number of nyquist diagram round the critical point (-1, 0) in a straight direction has to be equal to the instable zero number of its transfer function in open loop. In our application, the transfer function in open loop has no instable zero and as given in Fig. 7, its Nyquist diagram doesn't turn around the critical point in direct direction. Therefore, based on this criterion, the induction motor model is sable. Hence, the IMC can be used in the control loop.

Based on these five steps, the internal model controller is obtained and its recurrent equation is given by:

$$u(k) = b_0 e(k-1) + b_1 e(k-2) + a_0 u(k-1) \quad (32)$$

Where e is the error between real output and model output

$$a_0 = \alpha, \quad b_0 = \frac{1-\alpha}{a} \quad \text{and} \quad b_1 = \frac{(1-\alpha)b}{a}$$

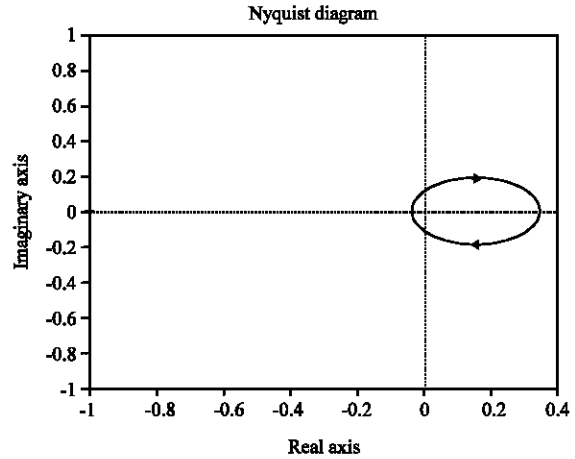


Fig. 7: Nyquist locality of the transfer function of the induction motor in the open loop

Experimental results: The bloc diagram of the control system that we realize experimentally using the ANN sensorless speed IMC is given in Fig. 8. It consists of the appropriate hardware and its software implemented through a processor based digital controller.

The major parts of the drive system are:

- An IMC Speed controller,
- An inverter drive,
- A power inverter based on the IGBT transistors (PWM of 5 kHz) and L, C filter,
- Current Hall sensors and speed tachogenerator,
- A scalar control set around a micro-controller,
- A PC with an acquisition (0.2 msec sampling time) and control card (voltage control: $\pm 10v$),
- An induction motor (1 kw-4.6A) coupled to a DC generator (1 kw-6.2 A) supplying a resistor tank.
- An artificial neural network speed observer implemented by the neural network toolbox from MATLAB (Heredia *et al.*, 2001).

The modulation frequency f_{PWM} is given by the following expression: $f_{PWM} = 48.f_s.Z$

Where Z is the repeated discrete point and f_s is the motor frequency.

To implement the ANN speed observer, the magnitude value of the stator current is needed. Assuming a set of balanced sinusoidal currents, the magnitude value, in terms of instantaneous quantities, can be written as:

$$I_s = \sqrt{\frac{4}{3}(i_{as}^2 + i_{as}i_{bs} + i_{bs}^2)} \quad (33)$$

Where i_{as} and i_{bs} are the stator currents measurements.



Fig. 8: A photo of the experimental set up

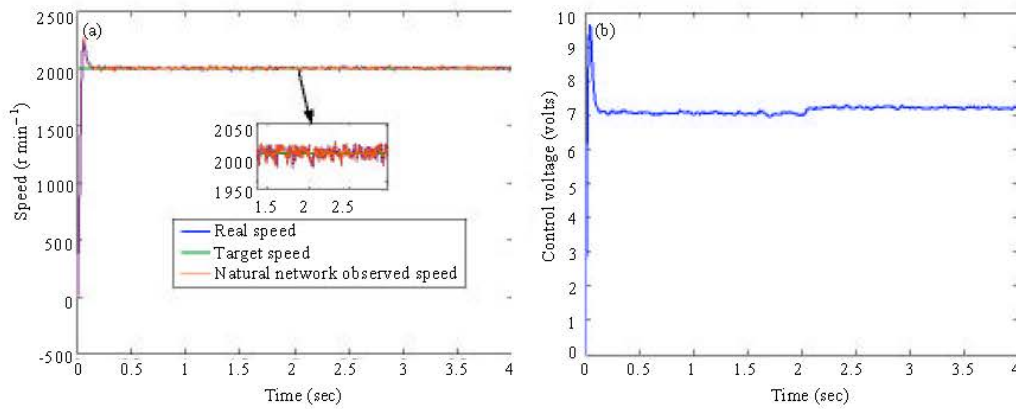


Fig. 9: Speeds and control voltage responses under constant load of 300 w

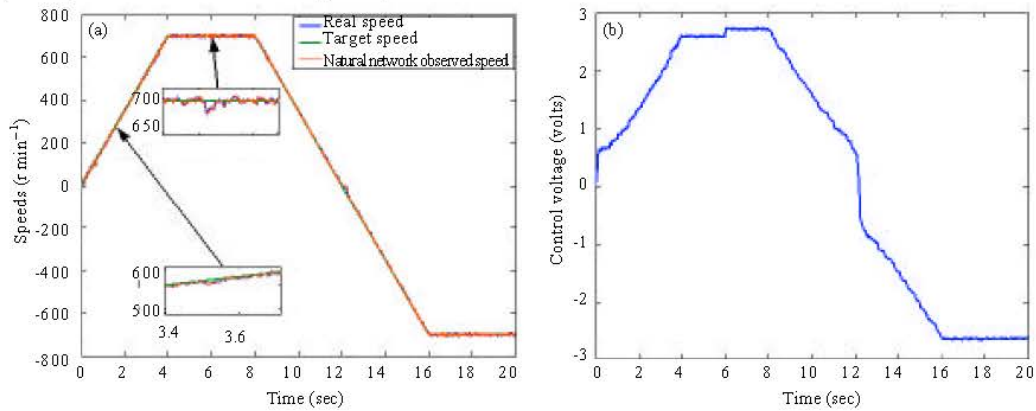


Fig. 10: Speed and control voltage responses of speed IMC controller under constant load of 300 w at $t = 3.5$ sec and 0.6 kw at $t = 6$ sec (variable target speed as acceleration and deceleration)

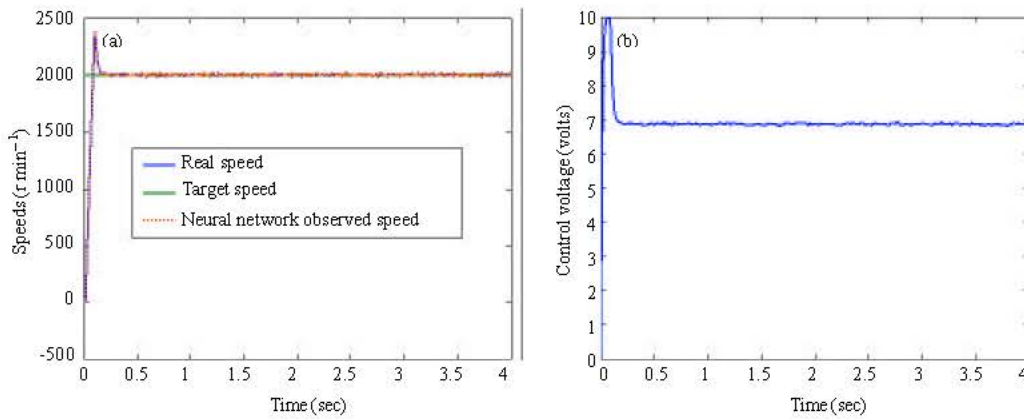


Fig. 11: Speed and control voltage under IMC controller (2000 r min⁻¹: field weakening region)

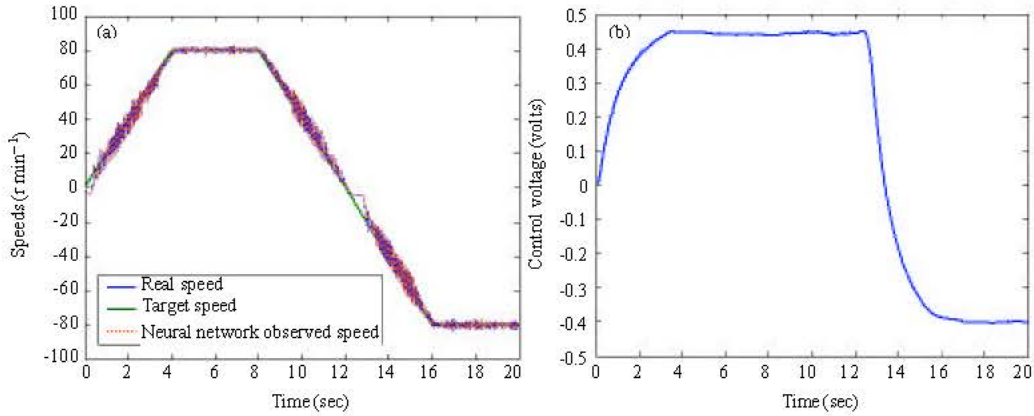


Fig. 12: Speed and control voltage under IMC controller (variable low target speed: Permanent target speed of ±80 r min⁻¹)

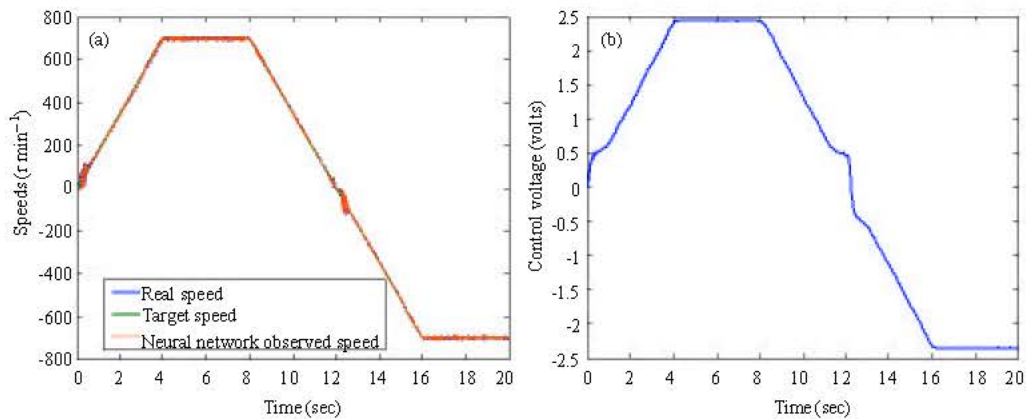


Fig. 13: Speed and control voltage under IMC controller (variable target speed ±700 r min⁻¹)

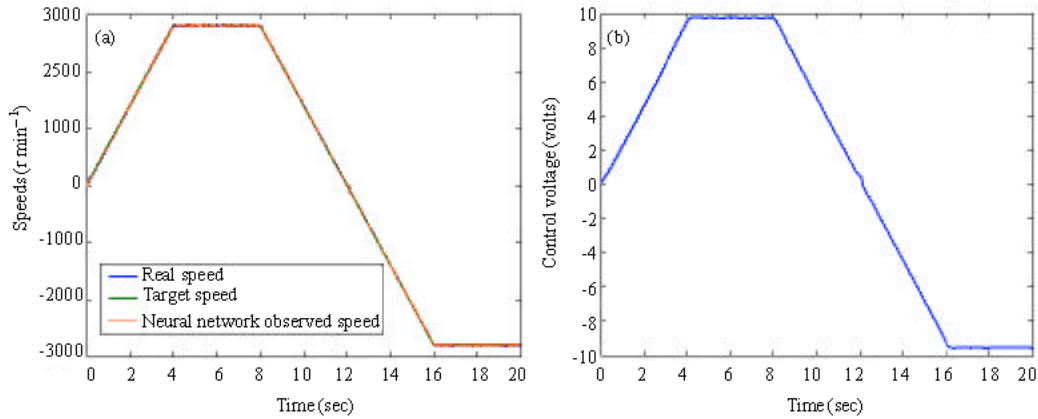


Fig. 14: Speed and control voltage under IMC controller (variable target speed: Field weakening region, permanent speed of $\pm 2800 \text{ r min}^{-1}$)

Many experiments were carried out under various operating conditions to verify the performance of the proposed ANN speed sensorless internal model speed controller (low speed operation, reverse operation, field weakening region, etc.) both with and without loading. Some selected results are presented in this section to highlight the significant operating conditions for the proposed system.

Figure 9 shows the step response for 2000 r min^{-1} with selected resistive applied load 300 W. These results justify the robustness of the overall control system under parameter variation and load disturbances.

In Fig. 10, a wide range of selected resistive loads is considered and applied in order to test the robustness of the sensorless speed proposed control algorithm. In this test, both dynamic and static states under load torque disturbance are considered. From these results, it is noted that the ANN speed observer and the IMC speed controller achieve good performance.

The tests of the algorithm under no load are given in Fig. 11-14. Low speed, field weakening region and reverse operation are all studied then tested experimentally. From these figures, it is seen that the proposed control algorithm has good performance and stability.

CONCLUSION

In this research, an internal model speed controller for induction motor is realized. An intelligent artificial algorithm developed in this investigation has been found capable of eliminating the mechanical speed sensor. An identification methodology based on the recursive least square algorithm is successfully applied in this study to

identify the parameters of the established mathematical model of the drive system. From the experimental results obtained using a 1kw induction motor drive system, it is shown that the proposed sensorless speed controller over the entire speed range and under a wide range of loads has a good performance and stability. The most important advantage of the proposed algorithm is the robust structure it provides and the simple and easy design it offers compared to other methods. The demonstrated effectiveness of the sensorless internal model controller in speed regulation and tracking, as robustness about parameter variations and external disturbances, implies that the internal model control can be extended to the regulation of such as the flux in the DSFO and DRFO strategies. This will be the subject of further studies.

REFERENCES

- Abdunnaser and J. Ali Milad, 2005. Competitive co-evolutionary design of robust internal model controllers to deal with prescribed large plant uncertainties. In: Proceeding of 3rd International Conference IEEE on Systems, Signals and Devices, 21-24, March 2005, Sousse, Tunisia.
- Ben, Y. Salem and L. Sbita, 2006a. H_∞ loop shaping applied to speed sensorless indirect stator field oriented control of induction motor drives. In: Proceeding of 4th international Conference IEEE on JTEA., 12 -14 December 2006 Hammamet, Tunisia.
- Ben Salem, Y. and L. Sbita, 2006b. A Non Linear State Feedback Control for Induction Motors. In: proceeding of IEEE on ICIT, 15-16 December, 2006, Monbey, India.

- Ben, M. Hamed and L. Sbita, 2006. Speed sensorless indirect stator field oriented control of induction motor based on luenberger observer. In: Proceeding of IEEE on ISIE, 9-13 July, 2006, Montréal, Canada.
- Borne, P. *et al.*, 1998. Control and Optimization of Process. Paris, France.
- Constantine, M. *et al.*, 2006. Thermal and slip effects on rotor time constant in vector controlled induction motor drives. IEEE Trans. Power Electron., 21: 495-504.
- Denai, M.A. and S.A. Attia, 2002. Fuzzy and neural control of an induction motor. Int. J. Applied Math. Comput. Sci., 12: 221-223.
- Dreyfus, C., 2002. Neural Network: Methodologies and Applications. Paris, France.
- Duc, G. and S. Font, 1999. H_∞ control and μ -analysis. Paris, France.
- Flaus, J.M., 2000. Industrial regulation: PID Controllers, Predictive and Fuzzy. Paris, France.
- Fonseca, J. *et al.*, 1999. Fuzzy logic speed control of an induction motor. Microprocessors Microsys, pp: 523-534.
- Grellet, G. and G. Clerc, 1996. Electrical Actuators. Paris, France.
- Heredia, J. *et al.*, 2001. Sensorless control of induction motors by artificial neural network. In: IEEE Trans. Ind. Applic., 48: 1038-1040.
- Hwan, S. *et al.*, 2001. Speed sensorless vector control of an induction motor using neural network speed estimation. In: IEEE trans. Ind. Applic., 48: 609-614.
- Jamie, A., A. Joaquin and R.J. Herrera, 1994. Internal model control for non linear systems: Application to an induction motor. Control Engineering Practice, 2: 1063-1066.
- Koubaa, Y., 2004. Recursive identification of induction motor parameters. Simulation Modelling Practice and Theory, 12: 363-381.
- Kubota, 1993. DSP Based Speed Adaptive Flux Observer of Induction motor. IEEE Trans. Ind. Applic., 29: 344-348.
- Lai, C.K. and K.K. Shyu, 2005. A novel motor drive design for incremental motion system via sliding-mode control method. IEEE Trans. Power Electron., 52: 7-30.
- Metwally, H.M.B. *et al.*, 2002. Proposed torque optimized behaviour for digital speed control of induction motors. Energy Convers. Manage., 43: 1675-1688.
- Oustaloup, A., 1994. Robustness: Analysis and synthesis of robust control. Paris, France.
- Sbita, L. and M. Ben Hamed, 2007. Fuzzy controller and ANN speed estimation for induction motor drives. In: Proceeding of 4th International Conference IEEE on Systems, Signals and Devices, 19-22, March 2007, Hammamet, Tunisia.
- Shao, X. *et al.*, 2005. Adaptive internal model control of permanent synchronous motor drive system. In: Proceeding of the 8th International Conference of Electrical Machines and Systems, 27-29 September 2005.
- Zidani, F., M.S. Nait Said, R. Abdessemed, D. Diallo and M.E.H. Benbouzid, 2002. A fuzzy technique for loss minimization in scalar-controlled induction motor. In: Proc. Conf. Electric Power Components Syst., 30: 625-635.